45th AIAA ASME
AIAA 2007-0572

Interaction of LOX/GH_2 Spray-Combustion with Acoustics

Bernhard Knapp, * Zoltan Farago†, Michael Oschwald‡
German Aerospace Center, Institute of Space Propulsion, Lampoldshausen, 74239 Hardthausen, Germany

The response of a cryogenic LOX/H_2-spray flame to acoustic pressure and velocity fluctuations has be investigated experimentally for pressure levels up to p=1MPa. The dimensions of the combustion chamber are chosen to have transversal acoustic modes at eigenfrequencies representative to full scale rocket combustors. A siren wheel periodically opening a secondary nozzle was used to excite pressure oscillations in the cylindrical combustor at levels up to p'/p~10%. It has been found that the secondary nozzle detunes the eigenfrequencies of the cylindrical resonator in a characteristic way. A 2D-modal analysis of the acoustic behavior of the resonance volume has been done and results agree very well with the experimental findings. By analyzing the temporal and spatial distribution of the flame response to the acoustic excitation the question is addressed whether there is a coupling of combustion and acoustics and whether this coupling is due to velocity or pressure sensitive processes. From the experimental data it is concluded that there is a positive coupling, and the coupling is due to pressure sensitive processes.

Nomenclature

d	=	diameter
I	=	intensity
I'	=	amplitude of intensity variation
J	=	momentum flux density
p	=	pressure
p'	=	amplitude of pressure variation
R_V	=	velocity ratio
v	=	velocity
We	=	Weber number
ρ	=	density
σ	=	surface density

I. Introduction

COMBUSTION instabilities are still a key issue in the development of rocket combustors after decades of extensive experimental and theoretical investigations[1,2]. The complexity of the various processes involved (liquid jet atomization, secondary atomization, droplet evaporation, kinetics, fluid-dynamical coupling of propellant domes and combustor etc.) and the interaction of these processes with acoustics still does not allow reliable modelling, simulation and predictions of stability margins.

Although various process are known to be candidates for a coupling of the acoustics to the combustion chamber processes, in general the basic mechanism due to which of these combustion processes energy is transferred into the acoustic wave is not known. As an example the acoustics may couple to the combustion due to pressure depended processes like droplet evaporation[3,4] or kinetics or it may couple through velocity dependent processes like for instance secondary atomization[5,6].

Modern intensified CCD cameras allow the acquisition of 2D intensity distributions with frame rates capable to resolve time scales typical for HF-instabilities in rocket combustors. Thus it is possible analyse the spatial distribution of the flame response in an acoustic field. When the combustor is acoustically excited on an eigenmode

* Head Combustion Instability Group, DLR Institute of Space Propulsion, 74239 Hardthausen, Germany.
† Combustion Instability Group, DLR Institute of Space Propulsion, 74239 Hardthausen, Germany.
‡ Head Rocket Propulsion, DLR Institute of Space Propulsion, 74239 Hardthausen, Germany.

the acoustic amplitudes are enhanced due to resonance and the acoustic field exhibits a well defined symmetry. Comparing the spatial symmetry of the flame response with the symmetry of the excited acoustic eigenmode allows relating the flame response with pressure or velocity nodes or anti-nodes. This approach gives access to the discussion whether acoustics and combustion are coupled due to a pressure sensitive or velocity sensitive process.
Results of a basic investigation of the response of a cryogenic LOX/H_2-spray flame to an acoustic excitation are presented in this paper. A combustion chamber with a geometry representative to full scale engines with respect to the frequencies of tangential eigenmodes is operated with liquid oxygen and hydrogen. LOX and GH_2 are injected into the combustor by a coaxial shear injector. The response of the spray flame to an acoustic excitation is investigated for a variety of injection conditions. By using different injector exit geometries and mass flows non-dimensional numbers like momentum flux ratios $J=(\rho v^2)_{H2}/(\rho v^2)_{O2}$, We-numbers $We=\rho_{H2}d_{O2}(v_{H2}-v_{O2})^2/\sigma$, and velocity ratios $R_V=v_{H2}/v_{O2}$ have been adjusted. The flame response is analyzed based on dynamic pressure recordings and high-speed visualization of the flame emission. The temporal resolved two-dimensional information on flame emission and the pressure field reconstructed from the dynamic pressure sensors are used to discuss the coupling of acoustics to combustion.

II. Experimental Set-up

A. Combustion Chamber

The combustion chamber CRC has a cylindrical shape with a diameter of R_{CRC}=20cm, thus the frequencies of the tangential eigenmodes in hot fire tests are in a representative range (1T ~4kHz). The length of the chamber is 4cm and as a consequence the longitudinal modes have eigenfrequencies far above the frequencies of the tangential modes of interest in this experiment. The chamber is shown in Figure 1.
16 ports in the cylindrical wall of the combustor can be equipped with various sensors or specific hardware. One port is equipped with a LN2-cooled injector head. LOX and GH2 are injected with a shear coaxial injection element in radial direction. In respect to the disk-like combustor volume and the radial injection of the propellants the concept of the set-up is similar to that used by Heidmann[7].
The exhaust gases are released through a main nozzle in axial direction. Using nozzles with different throat diameter and adjusting the mass flows tests can be done at pressures between 1.5 and 10 bar.
In one of the ports a secondary nozzle is mounted with a throat of 2mm diameter. The throat area ratio of the main nozzle to the secondary nozzle varies between 6 and 25, depending on the main nozzle diameter.
In the standard configuration the flame can be visualized by two small windows with 6cm diameter (see Figure 1). One is located at the location of injector exit and is used for high speed imaging of the spray flame. The other is used for optical access of a photomultiplier which has a higher dynamic range as compared to the CCD-camera. For specific measurements a huge window of 20cm diameter can be mounted giving optical access to the complete combustor volume.

B. Siren

A siren is used for the excitation of an acoustic oscillation at a well defined frequency in the combustor. The siren modulates the mass flow through the secondary nozzle and its rotational speed controls the excitation frequency.
During a test the excitation frequency is scanned with a slope of 500 Hz/s over the frequency range of interest.
The sonic throat of the secondary nozzle is connected to the combustor volume by a tube of about a quarter wave length of the 1T mode.
For a given position of the secondary wheel, an excited 1T-mode shows a fixed orientation of its pressure nodal line, which is oriented perpendicular to the axis defined by the orientation of the secondary wheel. By changing the port at which the secondary nozzle is mounted the orientation of the excited mode can be varied. Thus it is under control whether for example the pressure nodal line is near the axis of LOX/H_2 spray flame (Figure 2, right) or whether it is perpendicular to it (Figure 2, left).
In the right case of Figure 2 the spray is exposed only to a weak acoustic pressure oscillation and predominantly exposed to the influence of the transversal acoustic velocity field. The velocity vector is perpendicular to the spray axis and changes its sign twice a period. In the left case of Figure 2 the spray is exposed in the near injector exit region to maximum acoustic pressure oscillation and the acoustic velocity is zero at the injector exit. Downstream the spray axis the acoustic velocity is increasing and is directed parallel to the spray axis.

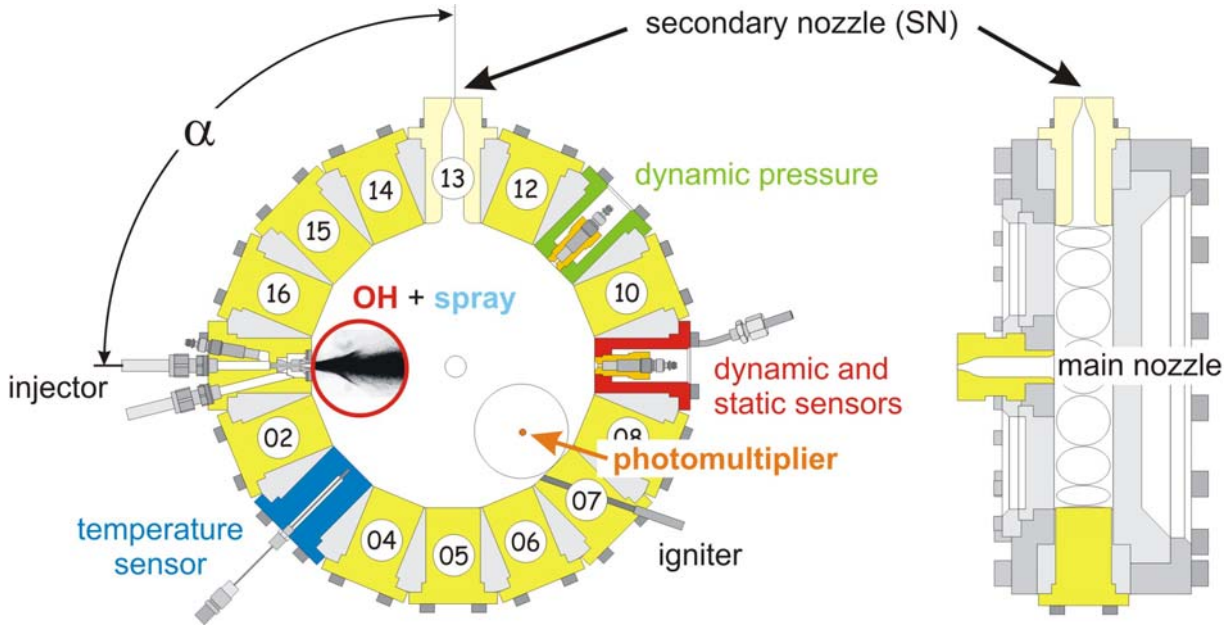

Figure 1: Combustion chamber CRC for HF-investigations.

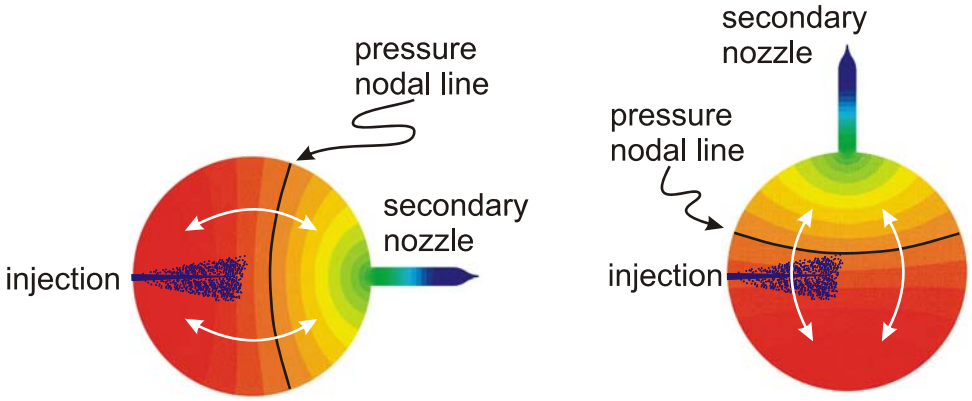

Figure 2: Pressure fields in the combustor. Left: secondary nozzle at the 90° port (pressure nodal line near to and parallel to LOX-spray), right: secondary nozzle at the 180° port (pressure nodal line perpendicular to the spray axis).

C. Sensors and Diagnostics

Static and dynamic pressure sensors are mounted in several ports to determine the level of acoustic excitation and to resolve the mode symmetry. The acquisition rate of the dynamic sensors was 27 KHz to meet the requirements of the Nyquist theorem for the modes of interest which have eigenfrequencies between about 4 KHz (1T) and 10 KHz (3T). Thermocouples flush mounted to the surface of the chamber wall are used to measure the surface temperature of the capacitively cooled combustion chamber.

The flame is visualized with intensified high speed CCD camera. With a Photron Ultima I2 (27000 frames/s, resolution 128x64 pixel) the flame emission was detected. Additionally a photomultiplier was used to measure locally the intensity of the flame emission. Both photomultiplier and high speed camera were equipped with an interference filter with a transmission at the wavelength of the OH-chemiluminescence near 307nm.

III. Experimental Results

A. Resonance Frequencies

The spectrum of eigenfrequencies of the cylindrical combustor equipped with the secondary nozzle shows significant differences as compared to that of a cylindrical resonator. Fourier transforms of the dynamic combustion chamber pressure without external excitation are shown in the left of Figure 3. The dynamic pressure exhibits

increased amplitudes on the eigenfrequencies of the acoustic system. The tangential modes 1T, 2T, the first radial mode 1R and higher modes can be clearly identified in the test without secondary nozzle. In the tests with secondary nozzle resonances near the frequencies of the cylinder modes are seen, however two resonances are observed near to the 1T-frquency. The other modes seems to be unaffected by the secondary nozzle.

The eigenfrequencies have been determined numerically for the acoustically coupled resonance volumes of the secondary nozzle's inlet tube and the cylindrical combustor. The eigenfrequencies as a function of the inlet tube length are shown in Figure 4. For an inlet tube with length $L/R_{CRC}=0$ the eigenfrequencies correspond to that of a cylindrical resonator. Due to the rotational symmetry of the cylindrical resonator the tangential modes are twofold degenerate, e.g. two independent eigenmodes exist with 1T symmetry with their pressure nodal lines perpendicular on each other. The secondary nozzle breaks the cylindrical symmetry and the tangential modes are no more degenerate. The 1T-modes split into two modes, one component has a pressure nodal line perpendicular to the axis of the secondary nozzle, the other mode has its modal line on this axis. The two components are labelled σ and π in Figure 4 respectively. With increasing L the frequency of the σ-component is decreasing whereas the frequency of the π-component is rather independent of the cavity length. For the π-component with its nodal line on the axis of the secondary nozzle, the additional volume of the nozzle's inlet tube is not participating in the acoustics and thus its eigenfrequency is not affected by the nozzle.

The length corresponding to the length of the cavity formed by the inlet tube of the secondary nozzle is plotted as a dashed line. As can be seen for this length 3 resonance frequencies are predicted with eigenfrequencies near to the 1T-frequency of the cylindrical resonator. The two resonances near the 1T-frequency seen in the spectrum of the combustor with secondary nozzle correspond to the 1Tσ and 2Tσ modes. A detailed analysis showed that the pressure sensor was located on a pressure nodal line of the 1Tπ-mode and the 1Tπ-resonance therefore could not be detected in this test. Furthermore from this analysis it became also clear why the resonance frequencies near the 2T- and 1R frequency were not affected.

The virtual splitting of the 1T-resonance when coupling an additional volume to the cylindrical combustion chamber volume has been observed first by G. Searby[9] in a similar set-up. Based on a 1D-modell he also was able to provide the basic understanding of the mechanism resulting in this splitting.

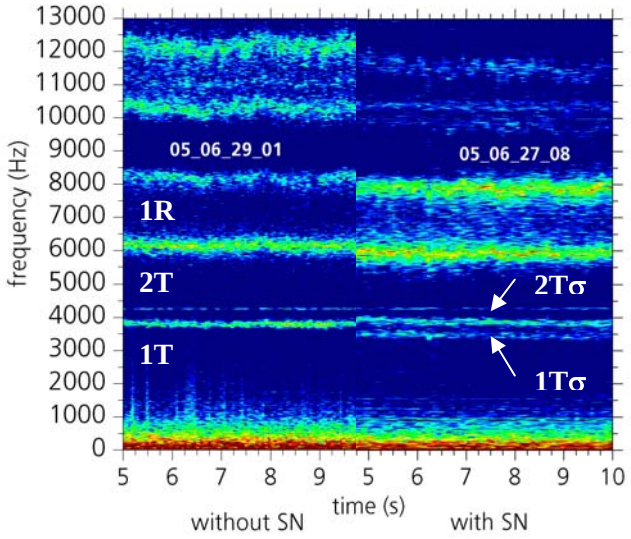

Figure 3: : Eigenfrequency of CRC with and without secondary nozzle (SN)

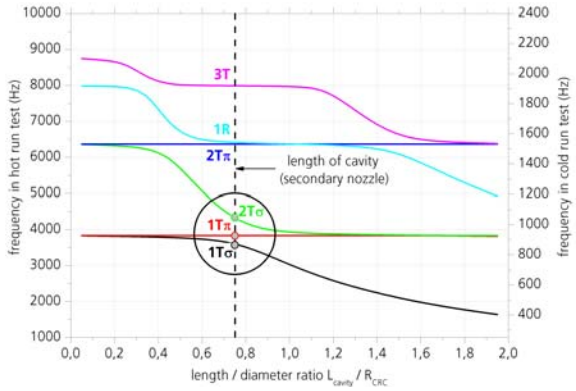

Figure 4: : Eigenfrequency of CRC with cavity as function of cavity length

B. Combustion Response to Acoustics

1. Coupling of heat release to acoustics

From the amplitudes and phases of the dynamic pressure signals the mode symmetry predicted by the numerical modal analysis (see Figure 7) could be confirmed. The pressure nodal line is nearly perpendicular to the axis of the exhaust tube of the secondary nozzle and the symmetry in the combustor reflects nearly 1T-symmetry.

The injection conditions of the liquid oxygen and gaseous hydrogen (mass flows, exit velocities) have been varied in a wide range. Momentum flux ratio *J* for instance was varied between 2 and 100. For a specific injection condition at the resonance frequency the amplitude of the dynamic pressure p' has been determined.
The response of the spray and the flame to the acoustic excitation is clearly seen in the high-speed visualizations. The periodic bending of the spray flame in the transverse acoustic field and the periodic modulation of the flame's OH-chemiluminescence I(t) at the resonance frequency demonstrate the interaction of the combustion process with the acoustic excitation. In Figure 5 a local measurement of the temporal evolution of the flame intensity is shown. It can be seen that the signal varies at low frequencies due to convective motion of flow volumes with high flame emissivity. A small HF-signal of amplitude I' at the frequency of the acoustic wave is superimposed. It has been proven, that the dynamic part of the flame emission I' oscillates in the limits of the measurement accuracy in phase with the acoustic pressure field p' (see Figure 6).

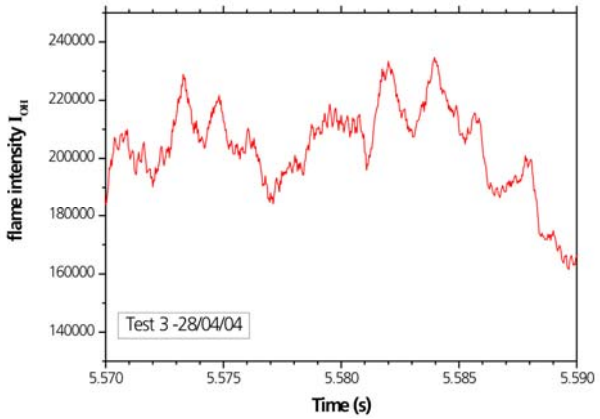

Figure 5: Temporal evolution of the flame intensity during external excitaion

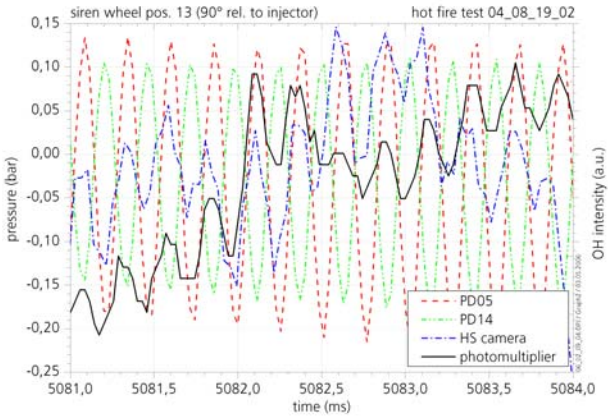

Figure 6: Phase relation between pressure and flame emission itensity

The chemiluminescence of the OH-radical I' is regarded as an indicator for heat release q'. The Rayleigh criterion requires that for a positive coupling of combustion and acoustics

$$\int_0^T p'q'dt > 0\,.$$

If the periodic variation of the heat release is identified with the flame emission I' and assuming harmonic time dependencies the criterion reduces to

$$p_0' \cdot I_0' \cdot \cos(\varphi) > 0$$

where φ is the phase shift between pressure and heat release. A phase shift φ=0 is therefore a proof for a positive coupling of the acoustics to combustion and energy of the combustion process should be transferred into the acoustic wave.
The sensitivity of rocket engines with respect to the appearance of HF-instabilities is known to be sensitive to the injection conditions of the propellants[8]. The injection conditions control for example the intact core length of the spray and the droplet size distribution. Thus it was expected for our experiment that the response of the heat release of the reactive spray on the acoustic excitation should be different for different injection conditions. With external excitation pressure levels p'/p of typically 10% have been obtained. However, no significant increase of the level of acoustic excitation p'/p has been observed in hot fire tests as compared to cold flow tests. and no correlation of the excitation level with one of the non-dimensional numbers *We, J, R_V* has been observed. Thus it has to be concluded, that any positive coupling of the spray flame to the chamber acoustics does not result in a gain. Energy transfer to the acoustic field due to the positive Rayleigh factor is balanced by damping effects of the set-up.

2. Pressure versus velocity coupling

The acoustic pressure and velocity fields have characteristic spatial distributions (see Figure 7) and the analysis of the flame emission response as a function of the orientation of the pressure nodal line is used to address the question whether the flame is coupled to the acoustic velocity or to the acoustic pressure.
Without secondary nozzle (and thus no external excitation) a low-level acoustic field is observed with 1T-symmetry and a pressure nodal line perpendicular to the injection axis (similar to the left sketch in Figure 2). Thus the mode

with maximum pressure oscillation in the injector near spray region is preferred. This is a first indication that energy from combustion is transferred into the acoustic 1T-mode by pressure coupling.

The relative oscillation of the chemiluminescence response I'/I with external excitation has been compared for the siren mounted at the 180°-position (left part of Figure 2) and the 90°-position (right part of Figure 2). The determination of I'/I showed some scatter from test to test for reasons not resolved today. Based on mean values from several tests it is concluded, that with external excitation a higher relative oscillation of the chemiluminescence response I'/I is observed in the spray with the siren at the 180°-port as compared to the 90°-excitation. Thus a higher dynamic response of the flame emission is induced when the pressure anti-node is in the spray region (as sketched in the left part of Figure 2). This is another indication for a pressure coupling of combustion and acoustics.

When the exciter wheel is mounted at the 90°-position the burning LOX/H_2-spray is very near to the pressure nodal line and exposed to transversal velocity fluctuations due to the acoustic excitation (see Figure 7). Thus in this configuration the coupling of the acoustic field to the spray region is due to velocity sensitive processes. In this case the direction of the velocity field is perpendicular to the spray axis and the velocity changes its sign twice per period. Because the velocity is perpendicular to the spray axis, an interaction of the velocity field with the spray should be independent of the sign of the velocity field and any velocity induced response should appear at twice the acoustic frequency. In all tests the Fourier component at 2ω is either not visible or smaller by at least an order of magnitude as compared to the ω-component. Therefore it is concluded that an eventual velocity coupling is small as compared to a pressure coupling.

The temporal evolution of the flame emission has been recorded by the intensified CCD-camera. The mean distribution for a test with the exciter wheel at the 90°-position is shown in Figure 9. Due to the limitation of the spatial resolution of the CCD-camera only the flame in the lower part of the combustor is visualized. The observed area is analyzed in sub areas as sketched in Figure 9. For each image the mean of the flame intensity in a sub area and from the image series its temporal evolution is determined. Thus the local mean $I_{mean}(x,y)$ and its amplitude fluctuation I'(x,y) at the excitation frequency could be evaluated. Correspondingly from the dynamic pressure recordings the amplitude distribution of the excited eigenmode is reconstructed.

In analogy to the response factor used by Heidmann and Weber[4]

$$N = \frac{\int_V \int_t^{t+T} p' q' \, dt dV}{\int_V \int_t^{t+T} p'^2 \, dt dV}$$

a local response factor N(x,y) is derived from the measured values I'(x,y) and p'(x,y):

$$N(x,y) = \frac{I_{\max}' / I_{mean}}{p_{\max}' / p_{mean}} .$$

In Figure 10a the mean value I_{mean} and in Figure 10b the amplitude I' of the flame emission is shown. Both distributions shown high values on the spray axis. Maximum variation of the flame emission I' is seen where the flame has maximum intensity. The relative flame response I'/ I_{mean} exhibits no maximum on the spray axis: near the pressure nodal line the relative I-variation is small and the maximum is observed where there is the pressure anti-node (see Figure 10). Thus the spatial distribution of I'/ I_{mean} reflects the pressure distribution of the excited 1T-mode.

From these observations it is concluded that for the conditions of the experiment there is coupling of the LOX/GH_2-spray flame to an acoustic wave and the coupling process is pressure sensitive.

The local response factor N(x,y) is shown in Figure 10d. Here a maximum is found on the spray axis, which is a very reasonable result, because sensitive processes (droplet vaporization, chemical reaction) are located in that region. However, whereas the results shown in Figure 10a-c are reproducible, the response factor derived from the data and shown in Figure 10d exhibits significant statistical error. The accuracy of the measurements has do be improved for a quantitative evaluation of N.

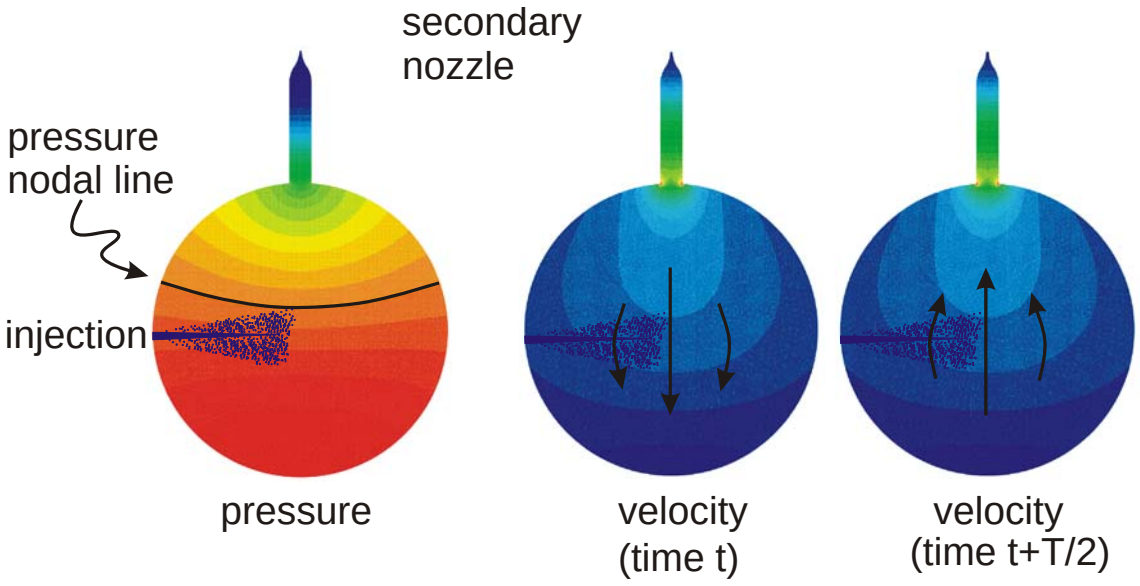

Figure 7: Acoustic pressure field (left) and magnitude of velocity (right) of the eigenmode of the combustor excited with the siren wheel a the 90° position.

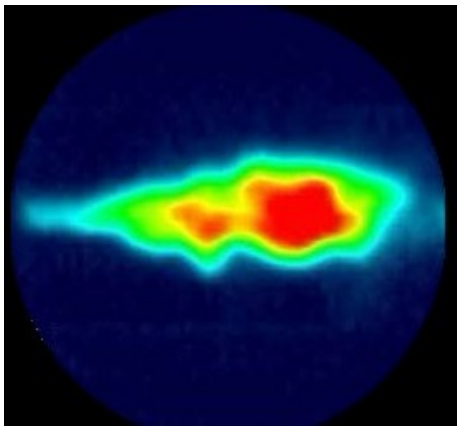

Figure 8: False colour representation of the OH-emission of the LOX/H2.spray flame observed through the small window (∅6cm) near the injector (see Figure 1).

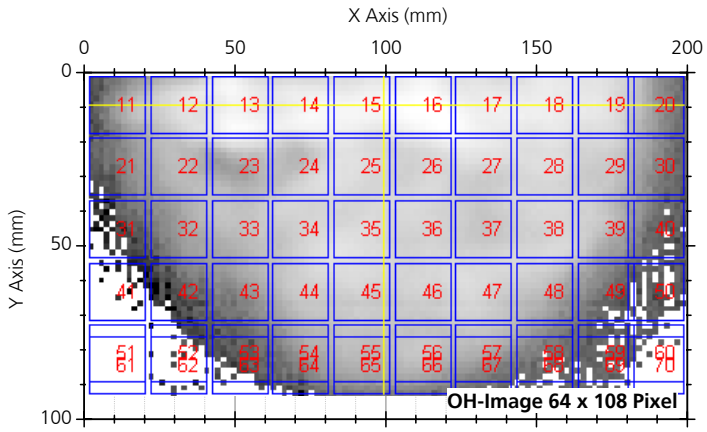

Figure 9: Mean flame intensity in the lower half of the combustion chamber with the exciter wheel mounted at the 90° position. The flame intensity is analyzed in sub areas of 10 pixel x 10 pixel size. The huge window (∅20cm) is used for optical access.

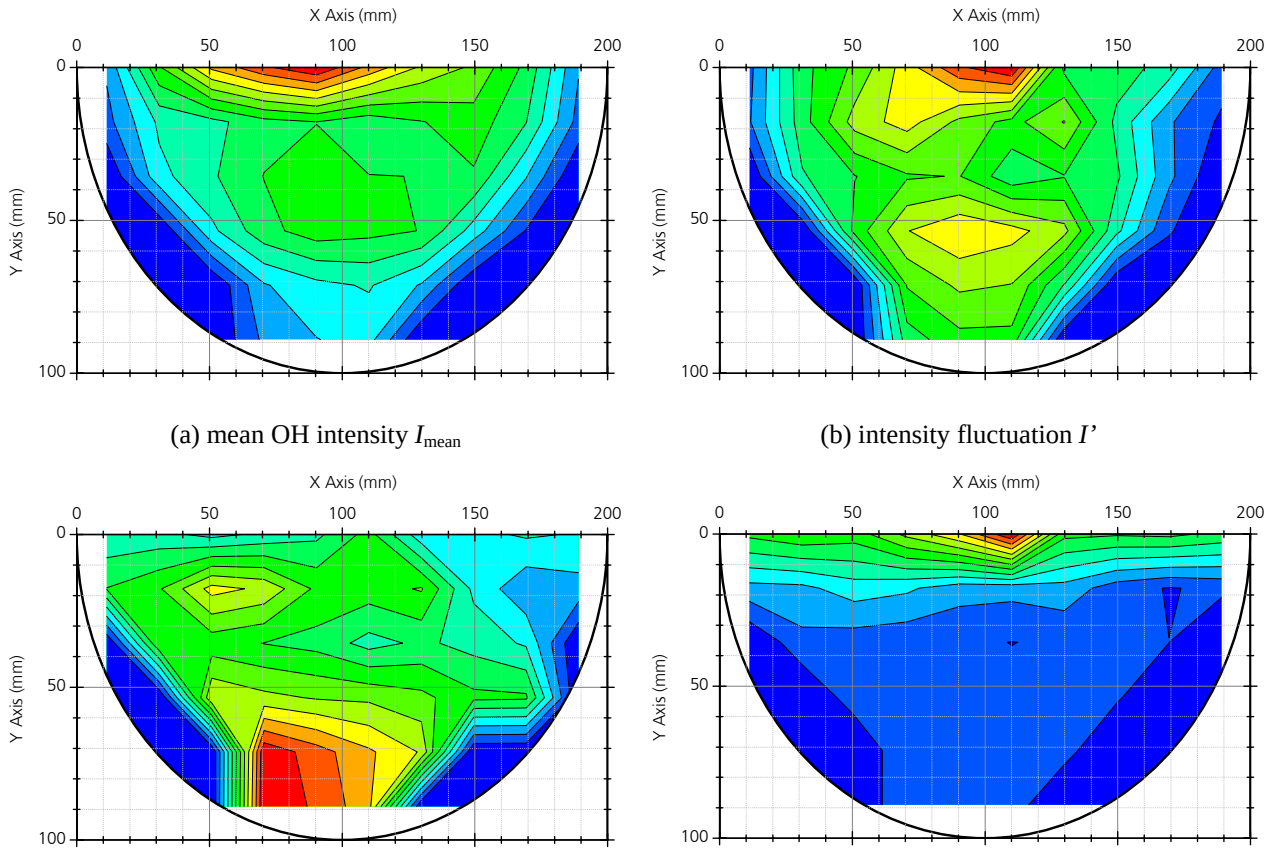

(a) mean OH intensity I_{mean}

(b) intensity fluctuation I'

(c) relative intensity fluctuation I'/I_{mean}

(d) response factor

Fig. 1

Figure 10: : Flame response during external excitation 90° relative to injector axis

IV. Summary

Based on the dynamic response of the flame emission to the acoustic excitation it can be concluded that a coupling of the acoustics to the spray combustion has been observed. According to the Rayleigh criterion the zero phase shift between dynamic part of the flame emission and the acoustic pressure indicates a positive coupling. However the experimental set-up did not allow realizing a coupling of heat release to the combustion process resulting in an increase of the acoustic amplitude.

From the behaviour of the local flame response for various orientations of the pressure nodal line for the excited mode it is concluded, that the acoustic field and the combustion process are coupled by a pressure sensitive process and not by a velocity sensitive process.

Acknowledgements

The authors are grateful to G. Searby from CNRS, Marseille, for his essential contributions to the understanding of the eigenfrequencies of the coupled acoustic system consisting of a resonance tube mounted to a cylindrical resonator.

References

[1]Harrje, D.T., Reardon, F.H. (Eds.), "Liquid Propellant Rocket Combustion Instability", *NASA, SP-194,* 1972

[2]Yang, V., Anderson, W. (Eds.), "Liquid Rocket Engine Combustion Instability", *AIAA Progress in Astronautics and Aeronautics*, Vol 169

[3]M.F. Heidmann, P.R. Wieber: Analysis of n-Heptane Vaporization in unstable Combustor with Travelling Transverse Oscillations; NASA TN D-3424, 1966

[4]M.F. Heidmann, P.R. Wieber: Analysis of Frequency Response Characteristics of Propellant Vaporization; NASA TN D-3749, 1966

[5]M.F. Heidmann, J.F. Groeneweg: Analysis of the Dynamic Response of Liquid Jet Atomization to acoustic Oscillations; NASA TN D-5339, 1969

[6]W.E. Anderson, K.L. Miller, H.M. Ryan, S.Pal, R.J. Santoro: Effects of Periodic Atomization on Combustion Instability in Liquid-Fueled Propulsion Systems, Journal of Propulsion and Power, Vol.14, No.5, 1998, pp. 818-825

[7]Heidmann M. F., "Oscillatory Combustion of a Liquid-Oxygen Jet with Gaseous Hydrogen", *NASA TN D-2753*, 1965

[8]Wanhainen J. P., Parish H. C., Conrad E. W., "Effect of propellant injection velocity on screech in 20000 pound hydrogen-oxygen rocket engine", *NASA, TN D-3373,* 1966

[9]Searby G., IRPHE, CNRS Marseille, private communication